Direct and indirect roles for Nodal signaling in two axis conversions during asymmetric morphogenesis of the zebrafish heart

Kari Baker*, Nathalia G. Holtzman†, and Rebecca D. Burdine*‡

*Department of Molecular Biology, Princeton University, Washington Road MOF433, Princeton, NJ 08550; and †Biology Department, Queens College, City University of New York, 65-30 Kissena Boulevard, Flushing, NY 11367

Edited by Clifford J. Tabin, Harvard Medical School, Boston, MA, and approved July 17, 2008 (received for review March 3, 2008)

The Nodal signaling pathway plays a conserved role in determining left-sided identity in vertebrates with this early left-right (L/R) patterning influencing the asymmetric development and placement of visceral organs. We have studied the role of Nodal signaling in asymmetric cardiac morphogenesis in zebrafish and describe two distinct rotations occurring within the heart. The first is driven by an asymmetric migration of myocardial cells during cardiac jogging, resulting in the conversion of the L/R axis to the dorsal-ventral (D/V) axis of the linear heart. This first rotation is directly influenced by the laterality of asymmetric gene expression. The second rotation occurs before cardiac looping and positions the original left cells exposed to Nodal signaling back to the left of the wild-type (WT) heart by 48 hours postfertilization (hpf). The direction of this second rotation is determined by the laterality of cardiac jogging and is not directly influenced by asymmetric gene expression. Finally, we have identified a role for Nodal signaling in biasing the location of the inner ventricular and outer atrial curvature formations. These results suggest that Nodal signaling directs asymmetric cardiac morphogenesis through establishing and subsequently reinforcing laterality information over the course of cardiac development.

asymmetry | southpaw | switch hitter | cardiac | rotation

Nodal signaling plays a conserved role in creating initial differences between the left and right sides of the vertebrate embryo. Alterations in early, left-specific expression of Nodal and its downstream targets results in abnormal organ placement and morphogenesis later in development (1). In zebrafish, the *nodal* gene *southpaw* (*spaw*) regulates the migration of the posterior lateral plate mesoderm (LPM) at the level of the gut tube and affects asymmetric budding of the liver (2). The nodal target *pitx2* has been shown to regulate the specification of the left atrium and asymmetric development of the outflow tract myocardium in the mouse heart (3, 4). However, there is little evidence of a direct function for Nodal signaling in the establishment of initial morphological asymmetries in the anterior LPM.

To address this question, we studied asymmetric cardiac development in zebrafish. The zebrafish heart undergoes two distinct asymmetric events. During the first process of cardiac jogging, a disk-shaped structure called the cardiac cone is converted to a linear heart tube by the repositioning of the atrial cells to the anterior and left of the ventricular cells (5, 6). These movements occur concurrently with asymmetric *spaw* expression in the left LPM. The second asymmetry, cardiac looping, is conserved in all vertebrates and positions the ventricle to the right of the atrium (5). In zebrafish, this process is initiated 10 h after *spaw* is expressed in the left LPM (7). We have examined both of these events and what role Nodal signaling plays in directing these asymmetries.

We find that the laterality of cardiac jogging is determined by a directional migration of left atrial cells within the cardiac cone and that this process is affected in mutants with altered asymmetric gene expression. These cellular movements result in a rotation of the cardiac cone and a conversion of the original left-right (L/R) axis of the cone to the dorsal-ventral (D/V) axis of the linear heart. We also describe a second rotation within the heart before cardiac looping that is not directly determined by asymmetric Nodal signaling. The consequence of this rotation is to reposition the original left cells back to the left of the heart. Finally, we have uncovered a role for Nodal signaling in establishing the sites of inner ventricular and outer atrial curvatures. Together, these results provide insights into the specific morphological changes occurring through asymmetric cardiac development and reveal multiple roles for the Nodal signaling pathway in establishing cardiac laterality.

Results

***lefty2* Expression Provides Evidence for Two Axis Conversions During Asymmetric Cardiac Morphogenesis.** Expression of *lefty2* in wild-type (WT) embryos is dynamic throughout cardiac development. Asymmetric *lefty2* RNA is initially visible in the heart at 18 hours postfertilization (hpf), remaining restricted to the left side until 22 hpf (Fig. 1*Aii*). From 22–28 hpf, *lefty2* expression changes and extends along the length of the heart tube (Fig. 1 *Bii–Dii*). At 29 hpf, *lefty2* expression becomes localized more significantly to the left side of the heart (Fig. 1*Eii*). By 30 hpf, *lefty2* RNA is restricted to the left side of the looping heart, with expression in the forming inner curvature of the ventricle and outer curvature of the atrium (Fig. 1*Fii*).

Temporal changes in *lefty2* expression coincide with cardiac jogging and the initiation of cardiac looping. To determine whether changes in localization of *lefty2* expression result from asymmetric morphogenesis, we performed a *lefty2* expression time course in *switch hitter* (*swt*) morphant embryos. *swt* mutants and morphants display defects in cardiac laterality (8, 9) as well as in earlier asymmetric gene expression (10) [supporting information (SI) Tables S1 and S2].

At 20 hpf, 53% of *swt* morphants exhibit reversed expression of *lefty2* in right cardiac cells (Fig. 1*Aiii* and Table S1). Considering the high correlation in percentages between morphants with right expression of asymmetric genes and those with reversed jogging directionality (Tables S1 and S2), it is likely that most, if not all, *swt* morphants with right jog exhibited an earlier right-biased expression of *lefty2*. At 22 hpf, embryos with right jog exhibit a change in *lefty2* localization, with expression now visible along the length of the heart (Fig. 1*Biii*). This expression

Author contributions: K.B., N.G.H., and R.D.B. designed research; K.B. and N.G.H. performed research; K.B., N.G.H., and R.D.B. analyzed data; and K.B., N.G.H., and R.D.B. wrote the paper.

The authors declare no conflict of interest.

This article is a PNAS Direct Submission.

‡To whom correspondence should be addressed. E-mail: rburdine@princeton.edu.

This article contains supporting information online at www.pnas.org/cgi/content/full/0802159105/DCSupplemental.

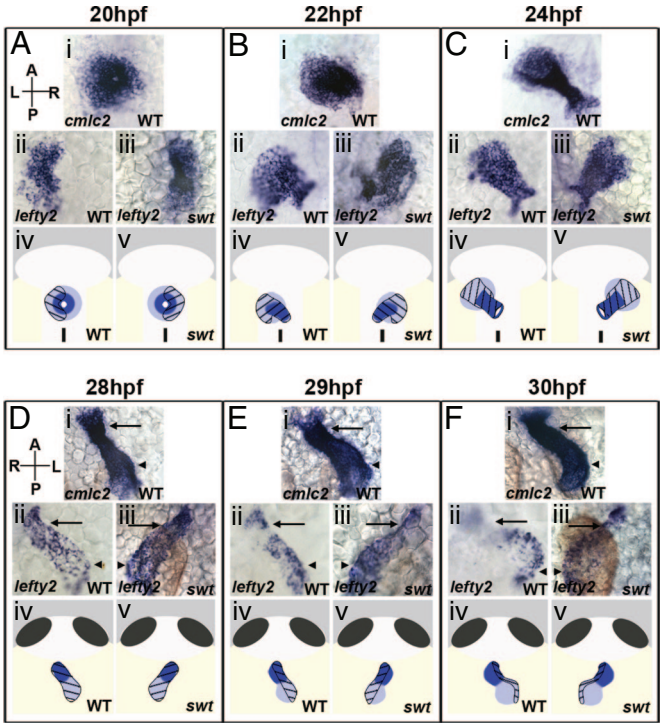

Fig. 1. *lefty2* expression temporally correlates with establishment of morphological asymmetries in the heart. Dorsal (*A–C*) and ventral (*D–F*) views of the heart from 20–30 hpf. Arrows indicate the ventricle and arrowheads the atrium (*Di–Fiii*). Cardiac cells were visualized by RNA *in situ* hybridization for *cmlc2*, expressed in all myocardial cells, and *lefty2*. In WT, *lefty2* expression is restricted to the left myocardium at 20 hpf (*Aii*), but extends symmetrically along the length of the left-jogged heart by 22–28 hpf (*Bii*, *Cii*, and *Dii*). A *swt* morphant exhibits reversed *lefty2* expression in the right myocardium (*Aiii*) at 20 hpf. At 22–28 hpf, *lefty2* is expressed along the length of the right-jogged heart in *swt* morphants (*Biii*, *Ciii*, and *Diii*). At 28–30 hpf, *lefty2* expression becomes restricted to the left side of the heart in WT (*Eii*) and is expressed exclusively along the left margin of the looping heart at 30 hpf (*Fii*). This process is reversed in *swt* morphants at 29 hpf. In this embryo, *lefty2* expression is still visible across the atrium (*Eiii*, arrowhead) but it restricted to the right side of the ventricle (*Eiii*, arrow). Right-sided localization is more pronounced by 30 hpf, with *lefty2* expression restricted to the right in both chambers (*Fiii*). The diagrams show atrial cells (light blue), ventricular cells (dark blue), localization of *lefty2* (black hatchmarks). L, left; R, right; A, anterior; P, posterior.

is similar to that observed in the left-jogged hearts of WT embryos (Fig. 1*Bii*). The later alteration in *lefty2* expression at 28–30 hpf is reversed in *swt* embryos with right-jogged hearts. In these embryos *lefty2* expression becomes concentrated on the right side of the heart (Figs. 1 *Eiii* and *Fiii*). In addition, the heart begins to loop in the opposite direction compared with WT, but with *lefty2*-expressing cells still present along the inner curvature of the ventricle and outer curvature of the atrium.

Asymmetric Migration of Atrial Myocardium Precedes Cardiac Cone Tilting. As changes in *lefty2* localization correlate with stages at which cardiac asymmetries are established, we questioned whether these changes are the result of relocalization of the left and right myocardium. We performed time-lapse imaging in *Tg*(*cmlc2:egfp*) embryos between 18–21 hpf to observe the movement of myocardial cells before cardiac jogging. In WT embryos ($n = 5/5$), at ≈19 hpf, the left atrial myocardium begins to migrate toward the left and anterior along the lateral edge of the cardiac cone (Fig. 2 *A*, *B*, *E*, and *F*; Movie S1). The right myocardium also initiates left-directed migration;, however, the predominant trajectories of right atrial cells are curved toward

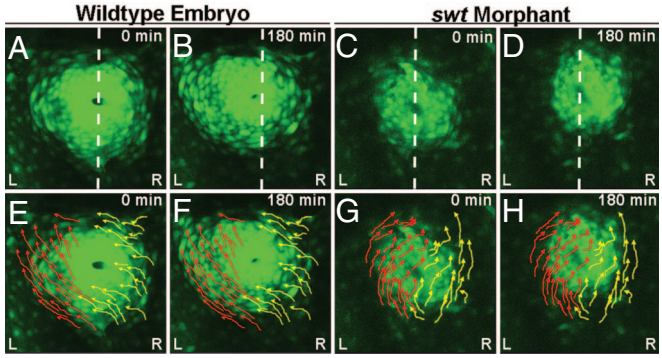

Fig. 2. Asymmetric atrial cell migration promotes rotation of the cardiac cone. (*A–H*) Dorsal views of the heart in *Tg*(*cmlc2:egfp*) embryos between 18–21 hpf. (*A–D*) Dotted white lines indicate the embryonic midline. (*E–H*) Arrows indicate trajectories of left (red) and right (yellow) cells. *A*, *E*, *C*, and *G* are the first frames of time lapses (0 min), and *B*, *F*, *D*, and *H* are the final frames (180 min). *A*, *B*, *E*, and *F* are frames from a time lapse of a single WT embryo, and *C*, *D*, *G*, and *H* are frames from a time lapse of a single *swt* morphant. In WT embryos, the left atrial myocardium migrates asymmetrically along the left of the cone toward the left and anterior (*E* and *F*). The right cardiac cells also migrate toward the anterior and left, but rather than sweeping along the lateral edge of the cone, these cells migrate toward the lumen (*E* and *F*). In *swt* morphants the L/R directionality of these cellular trajectories is reversed (*C*, *D*, *G*, and *H*). L, left; R, right.

the center of the cone rather than along the lateral edge (Fig. 2 *E* and *F*, Movie S1). The combination of these cellular movements results in the repositioning of the myocardium slightly to the left of midline and a clockwise rotation of the entire cone structure (Fig. 2 *E* and *F*; Movie S1). This rotation positions the left myocardium to the left anterior of the cardiac cone. Cone tilting occurs concurrently with the later stages of this migratory event, suggesting that atrial cell migration is responsible for repositioning the cone from the D/V axis to extending along the anterior-posterior axis.

To distinguish whether this asymmetry in migration is an inherent property of the myocardium or whether its laterality is controlled by asymmetric gene expression, we performed similar time-lapse imaging in *swt* morphants. Some morphants ($n = 4/9$) exhibited WT myocardial cell movements with a left-directed migration and subsequent left direction of cardiac jog. This result was expected given the high percentage of embryos with correct laterality of asymmetric gene expression (Table S1). In other morphants ($n = 3/9$), key aspects of cone morphogenesis, specifically the L/R identities of cells migrating along the lateral edge of the cone and of those migrating toward the center of the cone, are reversed (Fig. 2 *C*, *D*, *G*, and *H*; Movie S2). The cardiac cone in these morphants is also displaced to the right side of the midline, opposite of WT. Reversed L/R asymmetry of cell migration within the cone results in reversed cardiac jogging, with each of these morphants exhibiting a right directed jog. As right jog is correlative with right expression of *spaw* and *lefty2* earlier in development (8) (Tables S1 and S2), it is likely that the reversed atrial cell migration and cone tilting observed in *swt* morphants was preceded by right expression of Nodal pathway components in the LPM. This suggests that the laterality of Nodal signaling determines the direction of cell migration within the cardiac cone and indicates that cells exposed to asymmetric gene expression will migrate along the lateral edge of the cone, regardless of whether those cells originated in the left or right LPM.

Cardiac Jogging Converts the Original L/R Axis to the D/V Axis of the Linear Heart. The clockwise rotation of the cardiac cone in WT positions the left myocardium to the anterior of the right myocardium (Fig. 2*F*). This result, along with the change in *lefty2*

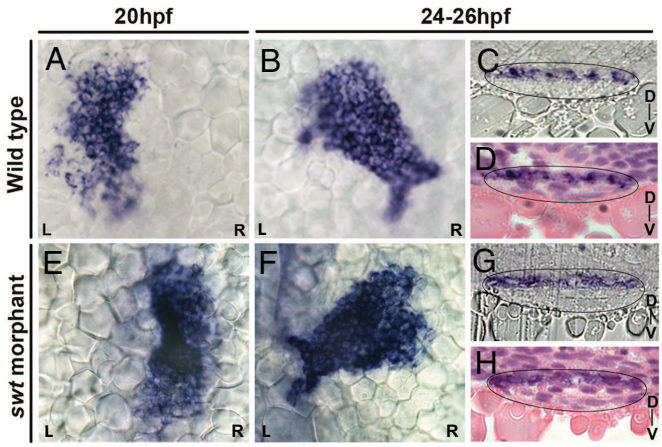

Fig. 3. Asymmetric cardiac jogging results in a L/R to D/V axis conversion. Shown are dorsal views of *lefty2* expression in the heart at 20 hpf and 24–26 hpf (*A*, *B*, *E*, and *F*) and in transverse histological sections at 24–26 hpf with heart tubes outlined in black (*C*, *D*, *G*, and *H*). Sections in *D* and *H* have been stained with hematoxylin and eosin. In WT, *lefty2* expression changes from left restricted expression at 20 hpf (*A*) to a symmetric extension at 24–26 hpf (*B*). Sections reveal that *lefty2* localization is restricted to the dorsal side of the heart (*C* and *D*). *swt* morphants that likely express *lefty2* on the right at 20 hpf (*E*) consistently display reversed cardiac jogging but also exhibit symmetric expression of *lefty2* along the length of the heart tube (*F*). However, sections reveal a dorsal localization of *lefty2* RNA, similar to WT (*G* and *H*). D, dorsal; V, ventral.

expression at 22 hpf from a left restriction to extension along the length of the heart, suggests that the left cardiac cells are repositioned to the dorsal side of the heart through the process of cardiac jogging. To confirm this L/R to D/V axis conversion, we examined the specific localization of *lefty2* expression in the heart at 24–25 hpf. Transverse histological sections through the heart tube at these stages reveal a restriction of *lefty2* expression to the dorsal side of the heart ($n = 6/6$) (Fig. 3 *C* and *D*). *lefty2* expression in WT, therefore, supports the existence of a L/R to D/V axis conversion occurring during cardiac jogging.

We next determined where the left and right myocardium would be localized along the D/V axis of the heart in *swt* morphants with reversed Nodal signaling and direction of cardiac jog. Transverse sections through right-jogged hearts of *swt* morphants reveal that *lefty2*-expressing cells within the heart tube are dorsally localized ($n = 6/6$) (Fig. 3 *G* and *H*). Therefore, although the morphological asymmetries of cardiac jogging are reversed in these embryos, the dorsal localization of *lefty2* within the heart tube after cardiac jogging is the same in both morphants and WT embryos. However, the important difference is that the dorsal cells in WT at 24 hpf originated in the left LPM, whereas dorsal cells in *swt* morphants originated in the right LPM.

A Leftward Rotation of the Heart Tube in WT Reestablishes the Original L/R Axis in the Heart at the Onset of Cardiac Looping. We observed a second change in *lefty2* RNA localization at the initiation of cardiac looping (Fig. 1 *Eii* and *Fii*), which we propose reflects a second axis conversion within the heart. We performed fate mapping experiments in WT embryos to track the left and right myocardial cells. The *Tg*(*cmlc2:dendra*) plasmid containing the GFP Dendra was injected into *Tg*(*cmlc2:dsredt4*) embryos (H.E. Riley and D. Yelon, New York University, New York). At 18–20 hpf, injected embryos were imaged, and those with GFP expression exclusively on one side of the myocardium were separated and individually tracked through 48 hpf.

WT embryos with left- or right-sided GFP expression at 18–20 hpf displayed GFP localization along the length of the heart at 24–28 hpf. Consistent with our histological analysis, embryos with early left-restricted GFP exhibited GFP localization on the dorsal side of the heart (Movie S3), whereas embryos with original right-restricted GFP exhibited GFP localization on the ventral side of the heart (Movie S4). This L/R to D/V axis conversion was observed in 100% of WT embryos examined ($n = 22$) (Table S3). When embryos with original left GFP were imaged again at 48 hpf, GFP-expressing cells were now restricted to the left side of the looped heart (Fig. 4 *A* and *A2*, arrowhead; Movie S5). In addition, we find that embryos with right-restricted GFP at 18–20 hpf display a subsequent right localization of GFP-expressing cells at 48 hpf (Fig. 4 *B–B3*, Movie S6). These results suggest that a leftward rotation occurs within the heart of WT embryos at the onset of cardiac looping to reposition the dorsal *lefty2*-expressing cells to the left of the heart (Fig. 4 *A1* and *B1*).

The Second Rotation Within the Heart Is Reversed in *swt* Morphants with Right Jog. We performed similar fate mapping experiments in *swt* morphants. *swt* morphants exhibiting the correct direction of cardiac jogging also displayed a WT localization of left and right cells along the D/V axis at 24 hpf (data not shown) and along the restored L/R axis of the looped heart at 48 hpf (Fig. 4 *C–C3*, Movie S7). These results are consistent with the 32% of *swt* morphants with the correct laterality of Nodal signaling and cardiac jogging/looping (Tables S1 and S2). Given the high correlation in percentages between right Nodal signaling in the LPM and right direction of cardiac jog, we were interested to determine the localization of the original left and right myocardium in the hearts of *swt* morphants with reversed jogging. Consistent with prior histological analysis, the left and right cardiac cells in 100% of these embryos exhibit reversed localization along the D/V axis at 24 hpf ($n = 18$) (Table S3). In right-jogged hearts, cells originating in the left myocardium become localized to the ventral surface of the heart, whereas cells originally present in the right myocardium become restricted to the dorsal surface of the heart (Movie S8 and Movie S9). The rotation of the heart tube at 28–30 hpf is also reversed in each of these embryos and is directed toward the right. *swt* morphants with left-restricted GFP at 18–20 hpf display a subsequent left restriction of these GFP-expressing cells to the left of the heart at 48 hpf (Fig. 4 *D–D3*, Movie S10). We find that these left cells in *swt* morphants with right-jogged hearts consistently contribute to opposite chamber structures compared with WT, being localized to the outer curvature of the ventricle (Fig. 4*D2*, arrow) and the inner curvature of the atrium (Fig. 4*D2*, arrowhead). Similar results were obtained by tracking embryos with right-restricted GFP expression (data not shown). These data suggest that reversed laterality of Nodal signaling and cardiac asymmetries lead to a reversed direction of heart-tube rotation at 28–30 hpf, similar to the reversal in cardiac cone rotation observed in *swt* morphants at 20 hpf.

The Direction of the Second Rotation Within the Heart Is Determined Independently of Nodal Signaling but Depends on the Direction of Jog. WT embryos with left jog exhibit a leftward rotation of the heart tube, whereas *swt* morphants with right jog display a rightward rotation. To clarify whether this reversal in heart-tube rotation is a direct consequence of reversed asymmetric gene expression, we performed fate mapping experiments in *spaw* morphants. These embryos lack expression of all asymmetric genes in the LPM and exhibit defects in cardiac laterality, including right-directed jog (7) (Tables S1 and S2).

Similar to WT, we find that *spaw* morphants with left-jogged hearts and original left expression of GFP exhibit dorsal GFP localization at 24 hpf (data not shown). These embryos also consistently position these GFP-expressing cells to the left of the looped heart at 48 hpf (Fig. 4 *E–E3*, Table S3, and Movie S11). Localization of left and right cells in *spaw* morphant hearts with

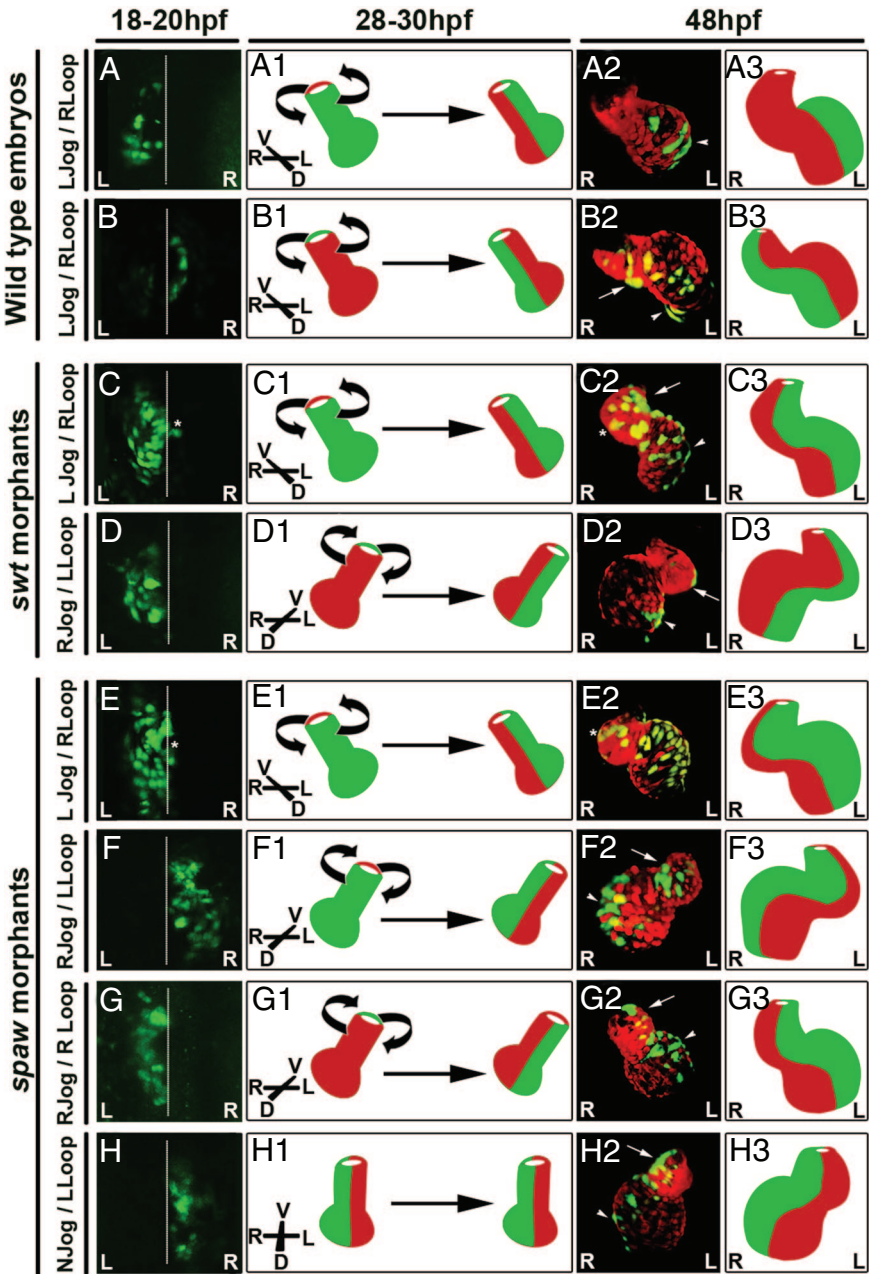

Fig. 4. A second rotation in the heart at 28–30 hpf converts the D/V axis back to the L/R axis. Cells are labeled with *cmlc2*::Dendra (green) and *cmlc2*::dsRED (red). *A*–*H* are dorsal views at 18–20 hpf; *A2*–*H2* are ventral views at 48 hpf. White lines indicate the embryonic midline. WT embryos with left (*A*) or right (*B*) GFP at 20 hpf display a left-directed rotation of the heart at 28–30 hpf (*A1* and *B1*). This rotation positions the original left cells from the dorsal side of the heart tube to the left of the looped heart (*A2* and *A3*) where they contribute to the outer atrial (*A2*, arrowhead) chamber curvature. The original right cells are repositioned from the ventral side of the linear heart to the right of the looped heart at 48 hpf (*B2* and *B3*) where they contribute to the outer curvature of the ventricle (*B2*, arrow) and the inner curvature of the atrium (*B2*, arrowhead). *swt* morphants with left jog and right loop display the same leftward rotation of the heart and contribution of original left cells to the inner ventricular (*C2*, arrow) and outer atrial (*C2*, arrowhead) chamber curvatures (*C*–*C3*). The asterisk in *C* marks GFP-expressing cells at 18 hpf that are to the right of midline. The asterisk in *C2* marks the likely localization of these cells at 48 hpf on the right side of the looped heart. *swt* morphants with left GFP at 20 hpf (*D*) and exhibiting right jog and left loop display a right-directed rotation of the heart at 28–30 hpf (*D1*). This rotation positions the left, GFP-expressing cells to the left of the 48 hpf heart (*D2* and *D3*) where they consistently contribute to the outer curvature of the ventricle (*D2*, arrow) and the inner curvature of the atrium (*D2*, arrowhead). *spaw* morphants with left jog and right loop display the same direction of heart-tube rotation and positioning of original left and right cardiac cells at 48 hpf as both WT and *swt* embryos with left jog and right loop (*E*–*E3*). The asterisk in *E* marks GFP-expressing cells at 18 hpf that are to the right of midline. The asterisk in *E2* marks the likely localization of these cells at 48 hpf on the right side of the looped heart. *spaw* morphants with right jog and left loop show the same reversed direction of heart-tube rotation as *swt* morphants with this phenotype (*F1*). In this embryo, the original right cells (*F*) are repositioned to the right of the heart at 48 hpf (*F2* and *F3*) and contribute to the inner curvature of the ventricle (*F2*, arrow) and the outer curvature of the atrium (*F2*, arrowhead). The same reversed direction of heart-tube rotation is observed in *spaw* morphants with right jog and right loop (*G1*). In this embryo, the original left cardiac cells (*G*) are positioned to the left of the heart at 48 hpf (*G2* and *G3*). These cells are localized to the outer curvature of the ventricle (*G2*, arrow) and the inner curvature of the atrium (*G2*, arrowhead). *spaw* morphants lacking directional jog also lack a directed rotation of the heart tube at 28–30 hpf (*H1*). *spaw* morphants with original right expression of GFP at 20 hpf (*H*) display a maintenance of these cells on the right of the heart at 24–28 hpf and at 48 hpf (*H2* and *H3*). In this embryo, the right GFP-expressing cells are localized to the inner curvature of the ventricle (*H2*, arrow) and the outer curvature of the atrium (*H2*, arrowhead). L, left; R, right; N, no; D, dorsal; V, ventral.

right jog and subsequent left loop was identical to that in the *swt* morphant hearts with the same phenotype. Cells originating in the right LPM became dorsally localized at 24 hpf (data not shown) and were subsequently positioned to the right side of the heart at 48 hpf (Fig. 4 *F*–*F3*, Table S3, and Movie S12). These results suggest that even in the complete absence of Nodal signaling, left-jogged hearts rotate toward the left, whereas right-jogged hearts rotate toward the right.

In contrast to WT and *swt* morphants, ≈20% of *spaw* morphants exhibit discordance between the directions of cardiac jogging and looping, with left jog resulting in left loop and right jog resulting in right loop (Table S2). These phenotypes provide the opportunity to question whether the correlation between these two asymmetric events influences the direction of heart-tube rotation. We find that *spaw* morphants with left expression of GFP at 18–20 hpf and right jog evident at 24 hpf still exhibit a reversed rightward rotation of the heart at 28–30 hpf even though the heart goes on to loop correctly to the right (Fig. 4 *G*–*G3*, Movie S13). Taken together, these data suggest that the rotation of the heart tube at the onset of looping is not directly influenced by the presence or laterality of Nodal signaling.

Another defect in cardiac laterality observed in *spaw* morphants is a lack of directionality in cardiac jogging, referred to as "no jog" (Table S2). We find that no-jogged hearts in *spaw* morphants exhibit two unique phenotypes. First, we observed that the repositioning of left and right cells to the D/V axis of the heart during cardiac jogging does not occur in *spaw* morphants with no-jogged hearts. Instead, cells originating in the left and

right LPM are retained on the left and right sides of the linear heart at 24 hpf (Movie S14 and Movie S15). Second, the no-jogged hearts of *spaw* morphants also failed to undergo heart-tube rotation at 28–30 hpf. However, because the earlier L/R to D/V axis conversion also failed to occur, the ultimate localization of left and right cells in these embryos was the same as that observed in WT, *swt* morphants, and *spaw* morphants with directional jog. Specifically, embryos with right GFP expression at 18–20 hpf exhibit a maintenance of GFP-expressing cells on the right of the linear heart at 24 hpf, and this right restriction is still evident at 48 hpf (Fig. 4 *H–H3*, Movie S16). This phenotype is observed in all embryos with no jog, regardless of GFP laterality at 18–20 hpf or subsequent direction of loop at 48 hpf (Table S3). These results suggest that the laterality of cardiac jogging directly determines the orientation of heart-tube rotation at 28–30 hpf, with the presence of directional jog being required for this rotation to take place.

Discussion

Our time-lapse imaging of WT embryos indicates the existence of asymmetric, left-directed migration of myocardial cells within the cardiac cone that ultimately results in a clockwise rotation of the cone before tilting. Similar time-lapse analysis done in *swt* morphants indicates that in a subset of embryos, the L/R directionality of these asymmetric events is reversed. Given the high correlation in percentages between right asymmetric gene expression and right jog in *swt* morphants, this phenotype is the likely morphological consequence of reversed Nodal signaling in the LPM (see model, Fig. S1 *A* and *B*). These data suggest that asymmetric gene expression guides the direction of atrial cell migration and, subsequently, the orientation of cardiac-cone tilt. It was recently reported that these asymmetric events preceding cardiac jogging are a consequence of the left-biased asymmetry in *bmp4* expression within the cardiac cone (11). In light of our data, it seems likely that Nodal signaling is upstream of *bmp4* expression in directing cardiac asymmetries. Alternatively, as the manipulations of BMP signaling described by these authors can affect the asymmetry of Nodal signaling within the myocardium, it is possible that *spaw* or *lefty2* more directly affect determination of cardiac laterality (11, 12).

Work by Rohr *et al.* (13) suggests that the direction of cardiac-cone tilt is a consequence of an asymmetric involution of right posterior myocardium, and that this site of involution is altered in *spaw* morphants. The authors propose that the process of involution itself occurs independently of Nodal signaling but that asymmetric gene expression is required to determine the site of this involution. The directed migration of posterior atrial cells that we observe in WT and *swt* morphants initiates just before the stage at which asymmetric involution is thought to occur. Consequently, our results indicate that the role for Nodal signaling in positioning the site of asymmetric involution may be through its earlier role in determining the direction of asymmetric atrial migration. This role for asymmetric gene expression would also explain why the site of involution is altered in the absence of Nodal signaling (13).

We find that asymmetric cell migration and the resulting rotation of the cardiac cone before jogging reposition the original L/R axis of the myocardium to the D/V axis of the linear heart by 24 hpf. In WT, the clockwise rotation of the cone and left direction of jog place the original left cardiac cells on the dorsal side of the heart (Fig. S1 *C* and *C1*). In *swt* morphants, a reversed, counterclockwise rotation of the cardiac cone followed by a right direction of jog results in the original left cardiac cells now being positioned on the ventral side of the heart (Fig. S1 *D* and *D1*). Importantly, despite the dorsal cells having originated in the right LPM of these *swt* morphants, the expression of *lefty2* in these cells at 24 hpf suggests that the right side of the myocardium, and not the left, had been exposed to Nodal signaling. These results indicate that cells exposed to asymmetric gene expression will invariably become localized to the dorsal side of the heart tube as an indirect consequence of the role for Nodal signaling in directing cell movements within the cardiac cone.

In addition to the rotation of the cardiac cone observed between 19–21 hpf, we have also described a second rotation within the heart at 28–30 hpf. Interestingly, the direction of heart-tube rotation is consistent with the direction of cardiac jogging in all embryos examined, including *spaw* morphants in which a lack of directional jog coincides with a lack of heart-tube rotation. In embryos exhibiting left jog, regardless of genotype, this rotation occurs toward the left (Fig. S1 *E* and *E1*). However, in *swt* and *spaw* morphants with right jog, the rotation is reversed and occurs toward the right (Fig. S1 *F* and *F1*). This consistency in the direction of rotation in right-jogged hearts regardless of the presence or absence of Nodal signaling indicates that this rotation is not directly influenced by asymmetric gene expression. Given this finding, it seems likely that the direction of heart-tube rotation is determined by a factor separate from, but doubtless affected by, L/R patterning. This influence might come either from within the heart itself or from a source extrinsic to the heart in the form of the vasculature or forces derived from blood flow through the chambers.

In WT and a number of mutant embryos, including *swt* morphants, the direction of cardiac jogging is predictive of and nearly always correlates with the direction of looping. In a WT situation, this means that left-jogged hearts consistently loop to the right, whereas in *swt* morphants, right-jogged hearts loop characteristically to the left. Interestingly, however, *spaw* morphants with right jog exhibit discordance between the directions of jog and loop. We find, in fact, that only 44% of the right-jogged hearts in these embryos loop to the left, compared with the 91% correlation between right jog and left loop observed in *swt* morphants. Consequently, a difference must exist between the right-jogged hearts of *swt* and *spaw* morphants to account for the different looping phenotypes observed in these embryos. Although it remains formally possible that the LRRC50 protein encoded by the *swt* locus performs a specific function within the myocardium, the lack of *lrrc50* RNA expression within the heart or myocardial precursors at any stage of development (9) indicates that this is likely not the case. As the earlier morphogenesis of right-jogged hearts is identical in both *swt* and *spaw* morphants, the only remaining difference that exists to explain the concordance of jog and loop in WT and *swt* morphants and the lack of concordance in *spaw* morphants is the presence or absence of Nodal signaling.

We show that in WT, left *lefty2*-expressing cells become localized to the dorsal side of the heart tube as a consequence of cardiac jogging. At the onset of cardiac looping, these cells are repositioned to the left side of the heart through a leftward rotation, where they consistently contribute to specific chamber structures through the process of dextral looping. Specifically, left ventricular cells form the inner curvature and left atrial cells form the outer curvature of the chambers. Importantly, these events are reversed in *swt* morphants exhibiting right jog. Through fate mapping analysis, we have shown that in these embryos the reversed direction of heart-tube rotation results in the right *lefty2*-expressing cells being positioned on the right side of the heart by 30 hpf. Despite having originated in the right LPM, these cells in *swt* morphants go on to consistently contribute to chamber structures characteristic of left-derived cells. Specifically, right cells within the ventricle form the inner curvature of the chamber whereas right cells within the atrium give rise to the outer chamber curvature. These results provide two insights into asymmetric cardiac morphogenesis. First, they indicate that the right myocardium of *swt* morphants with right jog exhibit a genetic left identity. Second, these data provide

evidence of a potential role for the Nodal signaling pathway in influencing the development of inner versus outer chamber curvatures (Fig. S1 *G* and *H*). Although the process of curvature formation is likely affected by other factors, including circulation, the laterality of Nodal signaling appears to bias the positions at which inner and outer curvatures form along the length of the heart tube.

A role for Nodal signaling in directly influencing the sites of curvature formations provides an explanation for why directions of jog and loop are so highly correlative in most embryos but become disconnected in *spaw* morphants. Although cardiac morphogenesis occurs identically in *swt* and *spaw* morphants with right jog, the left and right cells of *spaw* morphants completely lack specification of a genetic L/R identity. Consequently, no bias exists to consistently determine the sites of inner ventricular and outer atrial curvature formation, and this laterality decision is made randomly. As discrete chamber curvatures still form in most of these morphants, Nodal signaling cannot be responsible for directing the actual process of curvature development. Instead, asymmetric gene expression likely serves as a biasing mechanism to ensure that when these curvatures do form, they consistently develop at the same locations in every embryo.

It is important to note that, although not as consistently as in WT embryos, left-jogged hearts of *spaw* morphants do tend to loop correctly to the right. We believe this phenotype highlights the complexity and robust nature of cardiac laterality determination. It appears that once the initial bias in laterality is correctly established, even if this occurs in the absence of asymmetric gene expression, the chain of subsequent events that are normally indirectly influenced by Nodal signaling are sufficient to promote proper dextral looping. This finding suggests that the laterality of asymmetric gene expression is crucial to provide the initial bias in cardiac asymmetry but that once this process has been properly established, Nodal signaling is only moderately required to ensure that correct looping still occurs.

In consideration of our data, it appears that the Nodal signaling pathway plays multiple roles through the process of asymmetric cardiac morphogenesis and provides an intricate and elegant mechanism by which cardiac laterality can be coordinated and consistently maintained in a WT embryo. This is an indication that the Nodal signaling pathway may influence the direction of cardiac looping through differential specification or patterning of the left ventricular and atrial myocardium. In the future, it will be interesting to determine how Nodal signaling is able to bias the formation of chamber curvatures and what downstream targets of *spaw* might be involved in this process. In addition, it will be important to determine the mechanism controlling heart-tube rotation at 28–30 hpf, because this process is integral in WT embryos to position cells exposed to asymmetric gene expression to the proper side of the heart tube. Finally, future work should be directed toward a conclusive determination of whether Spaw, Lefty2, or BMP4 is the direct regulator of asymmetric cardiac development, or if an unknown, downstream component of the Nodal signaling pathway is the true effecter of laterality determination within the zebrafish heart.

Materials and Methods

mRNA, RNA Probes, and *in Situ* Hybridization. RNA *in situ* hybridization and transcription of mRNA and DIG-labeled antisense RNA probes were performed by using standard methods. The probes used were *cardiac myosin light chain* (*cmlc2*; *myl7*-ZFIN) (14), *lefty1* (15), *lefty2* (15), and *spaw* (7). The mRNA used was tol2 transposase (16).

Microscopy and Histological Analysis. Embryos analyzed by *in situ* hybridization were photographed as described (17). Embryos were processed for histological analysis as previously described (9). Time-lapse imaging and analysis was essentially performed as previously described (18). The Volocity program (Improvision) was used to create 3D reconstructions and movies. Detailed materials and methods for fate mapping and time-lapse analysis are provided in *SI Text*.

ACKNOWLEDGMENTS. We thank O. Grimm for the Dendra plasmid, H. E. Riley and D. Yelon for generously providing the *Tg*(*cmlc2:dsredt4*) before publication, J. Goodhouse for help with confocal microscopy, J. Sullivan-Brown for the *swt* morpholino, J. Schottenfeld and the members of the entire Burdine laboratory for discussions, and H. McAllister for zebrafish care. Some experiments were carried out on equipment from the Core Facilities for Imaging, Cellular, and Molecular Biology at Queens College. This work was supported by National Institutes of Child Health and Human Development Grant 1R01HD048584 (to R.D.B.).

1. Shen MM (2007) Nodal signaling: Developmental roles and regulation. *Development* 134:1023–1034.
2. Horne-Badovinac S, Rebagliati M, Stainier DY (2003) A cellular framework for gut-looping morphogenesis in zebrafish. *Science* 302:662–665.
3. Ai D, *et al.* (2006) Pitx2 regulates cardiac left-right asymmetry by patterning second cardiac lineage-derived myocardium. *Dev Biol* 296:437–449.
4. Shiratori H, Yashiro K, Shen MM, Hamada H (2006) Conserved regulation and role of Pitx2 in situs-specific morphogenesis of visceral organs. *Development* 133:3015–3025.
5. Glickman NS, Yelon D (2002) Cardiac development in zebrafish: Coordination of form and function. *Semin Cell Dev Biol* 13:507–513.
6. Stainier DY (2001) Zebrafish genetics and vertebrate heart formation. *Nat Rev Genet* 2:39–48.
7. Long S, Ahmad N, Rebagliati M (2003) The zebrafish nodal-related gene southpaw is required for visceral and diencephalic left-right asymmetry. *Development* 130:2303–2316.
8. Chen JN, *et al.* (1997) Left-right pattern of cardiac BMP4 may drive asymmetry of the heart in zebrafish. *Development* 124:4373–4382.
9. Sullivan-Brown J, *et al.* (2008) Zebrafish mutations affecting cilia motility share similar cystic phenotypes and suggest a mechanism of cyst formation that differs from pkd2 morphants. *Dev Biol* 314:261–275.
10. van Rooijen E, *et al.* (2008) LRRC50, a conserved ciliary protein implicated in polycystic kidney disease. *J Am Soc Nephrol* 19:1128–1138.
11. Smith KA, *et al.* (2008) Rotation and asymmetric development of the zebrafish heart requires directed migration of cardiac progenitor cells. *Dev Cell* 14:287–297.
12. Chocron S, Verhoeven MC, Rentzsch F, Hammerschmidt M, Bakkers J (2007) Zebrafish Bmp4 regulates left-right asymmetry at two distinct developmental time points. *Dev Biol* 305:577–588.
13. Rohr S, Otten C, Abdelilah-Seyfried S (2008) Asymmetric involution of the myocardial field drives heart tube formation in zebrafish. *Circ Res* 102:e12–19.
14. Yelon D, Horne SA, Stainier DY (1999) Restricted expression of cardiac myosin genes reveals regulated aspects of heart tube assembly in zebrafish. *Dev Biol* 214:23–37.
15. Bisgrove BW, Essner JJ, Yost HJ (1999) Regulation of midline development by antagonism of lefty and nodal signaling. *Development* 126:3253–3262.
16. Kawakami K, Shima A (1999) Identification of the Tol2 transposase of the medaka fish Oryzias latipes that catalyzes excision of a nonautonomous Tol2 element in zebrafish Danio rerio. *Gene* 240:239–244.
17. Schottenfeld J, Sullivan-Brown J, Burdine RD (2007) Zebrafish curly up encodes a Pkd2 ortholog that restricts left-side-specific expression of southpaw. *Development* 134:1605–1615.
18. Holtzman NG, Schoenebeck JJ, Tsai HJ, Yelon D (2007) Endocardium is necessary for cardiomyocyte movement during heart tube assembly. *Development* 134:2379–2386.